

The Effect of Average Soft Segment Length on Morphology and Properties of a Series of Polyurethane Elastomers.

II. SAXS-DSC Annealing Study

DARREN J. MARTIN,¹ GORDON F. MEIJS,² PATHIRAJA A. GUNATILLAKE,² SIMON J. MCCARTHY,² GORDON M. RENWICK³

¹The Cooperative Research Centre (CRC) for Cardiac Technology, Graduate School of Biomedical Engineering, University of New South Wales, Sydney, NSW 2052, Australia

²The CRC for Cardiac Technology, CSIRO Division of Chemicals and Polymers, Private Bag 10, Rosebank MDC, VIC 3169, Australia

³The CRC for Cardiac Technology, Department of Materials Science, University of Technology, Sydney, Broadway, NSW 2007, Australia

Received 16 July 1996; accepted 2 November 1996

ABSTRACT: A series of eight thermoplastic polyurethane elastomers were synthesized from 4,4'-methylene diphenyl diisocyanate (MDI) and 1,4-butanediol (BDO) chain extender, with poly(hexamethylene oxide) (PHMO) macrodiol soft segments. The PHMO molecular weights employed ranged from 433 g/mol to 1180 g/mol. All materials contained 60% (w/w) of the macrodiol. The materials were characterized by differential scanning calorimetry (DSC) following up to nine different thermal treatments. In addition, three of the materials were selected for characterization by small-angle x-ray scattering (SAXS) following similar thermal treatments. The DSC experiments showed the existence of five hard segment melting regions (labelled T1–T5), which were postulated to result from the disordering or melting of sequences containing one to five MDI-derived units, respectively. Evidence for urethane linkage dissociation and reassociation during annealing at temperatures above 150°C is presented. This process aids in the formation of higher melting structures. Annealing temperatures of 80–100°C provided the maximum SAXS scattering intensity values. Materials containing longer soft segments (and, therefore, longer hard segments) were observed to develop and sustain higher melting hard domain structures and also develop maximum average interdomain spacing values at higher annealing temperatures. Another additional series of three PHMO-based polyurethanes having narrower hard segment length distributions, was synthesized and characterized by DSC in the as-synthesized and annealed states. The resulting DSC endotherms provided further evidence to suggest that the T1–T5 endotherms were possibly due to melting of various hard segment length populations.

© 1997 John Wiley & Sons, Inc. *J Appl Polym Sci* **64**: 803–817, 1997

INTRODUCTION

DSC is a common tool used to determine the state of organization of molecules in a sample, for example, phase segregation, glass transitions, and

melting of crystalline regions. Typical thermal transitions observed in polyurethane elastomers may include the glass transition of either the “hard” or “soft” microphases, a short-range order endotherm of the hard phase attributable to storage or annealing effects, and endotherms associated with the long-range order of crystalline portions of either soft^{1–4} or hard segments.^{5–11}

The glass transition temperature of the soft mi-

Correspondence to: D. J. Martin.

© 1997 John Wiley & Sons, Inc. CCC 0021-8995/97/040803-15

crophase, $T_g(s)$, can be used qualitatively to indicate the amount of hard segment dissolved in the soft domains. A higher temperature $T_g(s)$ (compared with that for the pure soft segment) indicates an increased presence of hard segments dissolved in the soft domains.^{12,13} Any quantitative analysis involving $T_g(s)$, however, has been difficult for thermoplastic polyurethanes (TPUs) due to the complex morphology¹⁴ where the microdomain structure can impose restrictions on the motion of soft segments¹⁵ and where the soft domains can sometimes be partly crystalline.

The interpretation of the multiple endothermic behavior of TPUs remains an area of considerable interest. The size and position of melting endotherms have been shown to vary with changes in composition ratio,^{16–18} soft segment length,⁷ annealing,^{8,10,19,20} processing temperature,²¹ and mechanical deformation.²²

Of considerable interest have been the endotherms occurring between 50 and 250°C.

In earlier publications,^{17,23} the multiple endothermic behavior was attributed to either hydrogen bond distribution effects or to two types of hydrogen bonds, for example, hard segment interurethane hydrogen bonds and hard segment-soft segment hydrogen bonds.

More recent studies have shown that the DSC endotherms are not attributable to hydrogen bond dissociation. Samuels and Wilkes²⁴ prepared polymers very similar in composition to those previously characterized, but which employed hard segments based on piperazine and BDO. These materials lacked available hydrogen for hydrogen bonding, yet still displayed very similar DSC thermograms to those of the hydrogen-bonded materials. They proposed that the multiple endotherms were due to various levels of packing order in the hard domains.

Seymour and Cooper²⁵ supported this proposition by performing DSC annealing and variable temperature infrared studies on a series of polyether and polyester-based polyurethanes (ES and ET series). They labeled the various DSC peaks T_I , T_{II} , and T_{III} and attributed the T_I and T_{II} peaks to the disruption of short and long range order, respectively (due to the distribution in hard segment lengths), and the T_{III} peak to melting of microcrystalline order. The short range ordering could be continuously improved by annealing, manifest in the merging of the I and II regions. They also found that the thermal behavior of the hydrogen bonds was insensitive to the degree of ordering present and was affected primarily by the T_g of the hard segments. Above this T_g the

hydrogen bonds began to dissociate. Other IR studies have also reinforced this observation.^{26,27}

Ensuing studies by Wilkes et al.^{28–30} and Hesketh et al.⁷ concentrated on the kinetics of phase separation in melt quenching and annealing studies. These workers found that samples that were briefly heated to elevated temperatures (e.g., 170°C) and then rapidly quenched to room temperature exhibited decreases in $T_g(s)$, and increases in Young's Modulus as a function of time after quench. This indicated a time-dependent increase in the degree of phase separation (often termed demixing).

Van Bogart et al.¹⁰ performed an extensive DSC annealing study on several classes of TPUs and found that annealing at a certain temperature would invariably result in an endothermic peak 20–50°C above that annealing temperature. They also studied the response of an MDI/BDO hard segment polymer to annealing, and this yielded similar results to the block polymers containing shorter sequences of the same material. This suggested that annealing-induced ordering was an intradomain phenomenon and is not strongly dependent on the presence of soft segment phase.

Koberstein and co-workers^{20,31} used DSC and simultaneous SAXS–DSC to examine annealing induced changes in polyurethane morphology. The structure of the materials was analyzed by examining the relationships between the composition ratio, the presence and position of the various endotherms as shown by DSC, and the nature of the SAXS data. They found the existence of three endotherms, as previous investigators had also shown, and labeled them T_I , T_{II} , and T_{III} in keeping with previous nomenclature. It was shown that for a composition ratio of below approximately 50% by weight of hard segment that the hard segment domain was discrete. In this region (where the hard domain was discrete) two endotherms were observed (T_I and T_{II}). The T_I endotherm was found to occur at approximately 20 degrees above the annealing temperature and was attributed to a local reorganization within the hard domain. The T_{II} endotherm was found generally in the range of 140–200°C. The onset of the T_{II} endotherm was found to be coincident with a dramatic shift in the long-spacing observed in SAXS experiments. Based on these observations, they assigned the origin of this peak to the microphase separation transition (MST), which was associated with the microphase mixing of “noncrystalline” hard and soft segments. A further endotherm (above 200°C) was found in samples that had a continuous hard microdomain

structure. This T_{III} endotherm was ascribed to melting of the microcrystalline region in the hard-segment-rich microphase.

At this point there was still a discrepancy as to whether the T_{II} endotherm was actually a "MST" or whether it involved the instantaneous mixing of hard and soft segments during disordering of regions including "paracrystalline" (imperfect crystallites) hard segments.

The Koberstein–Stein "partial miscibility" morphological model^{31,39} was developed at around this time to accommodate the following important observations.

1. The glass transition of the soft microphase, $T_g(s)$ has been shown to increase with increasing annealing temperatures observed in DSC and DMTA studies, suggesting a higher degree of hard-soft segment mixing.^{12,13}
2. The high-temperature multiple melting endotherms observed in MDI/BDO-based TPUs (i.e., T_{II} and T_{III}) are shifted to slightly higher temperatures with increasing annealing temperature, suggesting an increase in the average length of the hard segments involved.^{10,20,25,31}
3. There exists an absence of extensive long range order in WAXD studies of typical TPU elastomers based on MDI-BDO hard segments.^{3,36,55,57,58} That is, strong diffraction patterns have only been obtained from hard segment model compounds,^{6,33,35,38,44–48} from stretched, heat-set TPUs⁴⁹ and TPUs involving a high fraction of hard segments (>50% by weight).
4. Hard domain thickness (estimated using SAXS) increases slightly with increased annealing temperature, but does not vary linearly with the calculated average hard segment length.^{11,39}
5. Synthesis of TPUs normally produces a material with quite a broad hard segment length distribution,^{40,41} meaning that the development of "ideal" hard segment crystals as reported for some monodisperse model compounds is less likely in a TPU elastomer prepared in the usual manner.

This model^{31,39} allows for both extended and coiled/folded hard segment conformations and it explains that for a given annealing temperature there will be a tendency for intermediate-length sequences to crystallize preferentially. As the annealing temperature is increased, the critical

length for hard segment dissolution increases, and increased mobilities permit crystallization of successively longer hard segment sequences. Hard segments shorter than this critical length are dissolved in the soft domains.

The upper limit for this "most-readily-crystallizable" sequence length distribution is the thickness of the lamellar hard domains (estimated to scale between two and four hard segment repeat units,^{11,39} depending on the formulation). Hence, morphological constraints cause hard segments longer than the hard domain thickness to kink and reenter the hard domains, thus impeding their ability to crystallize effectively. It was proposed that the longer hard blocks could fold back into the crystalline lamellae through the introduction of *gauche* conformations into the butanediol residue. Further support came for this theory when Koberstein and his co-workers^{42,43} used solid-state deuterium NMR on a MDI-butanediol-2,2,3,3,*d*⁴ polymer. They examined the rate, angular range, and the nature of motion of the BDO residue to find that it was present in various conformations (*gauche* and *trans*) and did switch between these conformations at a rate that was determined by the temperature of the sample. Hence, it was probable that the BDO residue could facilitate folding or coiling as per the proposed Koberstein model.

Several workers have approached the problem of understanding TPU structure and properties by synthesizing hard segment model compounds and polyurethanes with monodisperse hard segments.^{6,21,33,35,38,44–47,50–54} In 1986 Eisenbach and co-workers⁵⁰ employed both of these approaches in a thorough study that complements this study very nicely. The outcomes of some of this work shall be compared and discussed below.

In this SAXS–DSC annealing study, a series of polyurethanes with small, systematic changes in average segment length was characterized after undergoing several different thermal treatments. This was carried out in an effort to elucidate the origin of multiple melting endotherms commonly encountered in DSC thermograms of polyetherurethanes incorporating MDI-BDO hard segments. In a previous study³⁶ involving morphological and physical characterization of this same series annealed at 135°C only, four DSC melting endotherms of interest were encountered and these were labelled T1, T2, T3, and T4. The results provided enough evidence to hypothesize that these four endotherms were a result of the disordering of structures including predominantly single MDI-derived sequences, MDI₂BDO-, MDI₃BDO₂-, and MDI₄BDO₃-derived

Table I Molar Ratio of Ingredients for First PU Series

Material	PHMO (mol)	MDI (mol)	BDO (mol)
H433	1.0	1.1	0.1
H476	1.0	1.2	0.2
H650	1.0	1.6	0.5
H708	1.0	1.7	0.6
H793	1.0	1.8	0.8
H851	1.0	2.0	0.9
H998	1.0	2.3	1.2
H1180	1.0	2.6	1.5

hard segments, respectively. It was also proposed that the sometimes broad T2 endotherm may also be associated with the disordering of folded, longer hard segments.

In this article an additional series of three materials with controlled hard segment length populations was also prepared, and these materials were examined by DSC to enable further clarification of the abovementioned propositions.

The results from any characterization by DSC of high-temperature thermal transitions and of polyurethanes that have been annealed at high temperatures require careful interpretation. This is due to the limited thermal stability of the MDI/BDO urethane linkage at temperatures above 160°C.^{6,32–35} Further evidence of this phenomena is also presented and discussed in this article.

EXPERIMENTAL SECTION

Materials Preparation

Series Involving Variation in Average Segment Length

The methods employed for the synthesis and compression molding of the eight polymers in the series are detailed in Part 1 of this work.³⁶ The molar ratio of ingredients for these polymers are given in Table I.

Annealing was carried out on predried sheets/plaques (0.1 Torr at 40°C overnight) under a dry nitrogen purge at 80, 100, 120, 135, 150, and 170°C for 10 h, and these sheets were allowed to cool to room temperature over several hours in the oven. Samples of H851, H998, and H1180 were exposed to additional thermal treatments of 185 and 200°C for 10 h for DSC characterization only. Materials were also tested in the as-molded state.

Series Involving Narrower Hard Segment Sequence Length Distributions

An additional series of three polyurethanes involving a fixed PHMO soft segment length and variation in hard segment length was prepared. The hydroxyl number of the PHMO macrodiol was determined by a standard procedure (ASTM D2849-method C, 1975)³⁷ and gave a molecular weight of 696 g/mol. The molar ratio of ingredients for these polymers are given in Table II.

Single MDI Hard Segment Polymer (M1)

Equimolar amounts of dried (better than 0.1 Torr at 105°C for at least 12 h) PHMO and distilled MDI were reacted together in a plastic beaker. The polymer was cured in the beaker at 100°C for 4 h under a steady flow of dry nitrogen.

MDI–BDO–MDI Hard Segment Polymer (M2)

First, a prepolymer was made by end-capping 1 mol of PHMO with 2 mol of MDI. The MDI was weighed into a reaction flask fitted with a magnetic stirrer bar, nitrogen inlet, and an addition funnel. The reaction flask was placed in an oil bath at 70°C and the molten, dried macrodiol was then added slowly from the addition funnel over a period of 10 min and reacted for a total time of 2 h while stirring and under a steady dry nitrogen flow. One hundred grams of this prepolymer was then accurately weighed out into a plastic beaker. An equimolar amount of BDO was added to the prepolymer and this reaction mixture was stirred continuously with a spatula for 2 min to ensure uniform mixing of all ingredients. The polymer was cured in the beaker at 100°C for 4 h under a steady flow of dry nitrogen.

Longer Hard Segment Polymer (M3/M5)

In this case a polymer containing a reasonably well-known distribution of longer hard segment

Table II Molar Ratio of Ingredients for Second PU Series

Material	PHMO (mol)	MDI (mol)	BDO (mol)
M1	1.0	1.0	0.0
M2	1.0	2.0	1.0
M3/M5 ^a	1	4	3

^a Theoretical values.

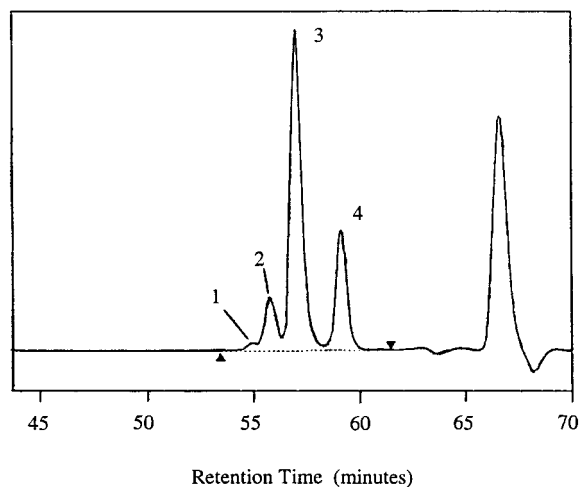


Figure 1 Gel permeation chromatograph of mixture containing approximately equal fractions of “B2” and “B4” compounds (indicated by peaks labeled 3 and 4, respectively), as well as small amounts of some higher fractions indicated by peaks labeled 1 and 2.

sequences that included mainly three and five MDI units per hard segment was synthesized. A mixture containing mostly BDO–MDI–BDO (B2) and BDO–MDI–BDO–MDI–BDO–MDI–BDO (B4) was synthesized via a method similar to that used by Christenson et al.³⁸ A solution of 210 g (0.84 mol) of MDI dissolved in an equal volume of *N,N*-dimethylformamide (DMF) was added to a solution of 600 g (6.7 mol) of 1,4-butanediol with stirring and heating at approximately 50°C for 2 h.

The mixture was left at ambient temperature overnight. Crystals that formed were collected by filtration and washed first with methanol and then several times with distilled water to remove DMF. The white compound obtained was dried to constant weight in a vacuum oven held at 110°C. Hydroxyl end-group analysis indicated a molecular weight of 650, which is between that of B2 (430.50) and B4 (861.00). GPC of this compound displayed two primary peaks (shown in Fig. 1), which had number average molecular weights of 1441 and 787, respectively (polystyrene equivalent). The compound also possibly contained small amounts of higher fractions as shown by the small GPC peaks labeled ‘1’ and ‘2.’ Determination of molecular weights was made difficult due to poor baseline separation. However, taking into account the average molecular weight of the compound (650 by OH #) and the observation of two primary peaks in the chromatograph, it was reasonable to assume that it was predominantly

made up of B2 and B4 molecules, with approximately even numbers of both.

To synthesize the “M3/M5” polyurethane, 100 g of prepolymer (polyol end capped with MDI) was accurately weighed out into a plastic beaker. In a separate plastic beaker an equimolar amount of the dry “B2/B4” compound was weighed out and dissolved in approximately 100 mL of DMF solvent and added to the prepolymer. The mixture was stirred well for 2 min before pouring onto a flat tray and placing into an oven at 100°C for 24 h with a strong purge of dry nitrogen to remove the solvent. To ensure thorough solvent removal the resulting sheet of polymer was chopped into very small pieces and soaked in a large container of distilled water with stirring, before being dried in a vacuum oven at 50°C.

Apart from a smaller percentage of “single MDI”-derived units that are known to result from the prepolymer synthesis (often termed “prechain extension”), and a small fraction of hard segments that included more than five MDI-derived units, it was believed that the polymer included a basically bi-modal distribution of hard segment sequence lengths including either three or five MDI-derived units per sequence. It was estimated that there were approximately equal fractions of both hard segment lengths.

The M1 polymer is in fact an alternating MDI–PHMO block copolymer including no BDO and is composed of 26.4% (w/w) of MDI.

Hard segments in the M2 material are almost totally made up of the MDI–BDO–MDI type, and this material has a composition ratio of 45.9% (w/w) hard segment.

In the case of M3/M5, this polymer virtually contains a bi-modal distribution of hard segments of either three or five MDI groups per hard segment. The estimated amount of each type of hard segment is approximately 50%. The M3/M5 polymer has a composition ratio of 62.3% (w/w) hard segment.

Instrumentation and Methods

For the series involving variation in average segment length, DSC measurements were performed on a Mettler DSC-30 with a 10°C/min heating rate. DSC samples were dried (0.1 Torr at 40°C overnight) prior to testing, and a sample weight of about 10 mg was used. Annealing was carried out on predried samples (0.1 Torr at 40°C overnight) in an oven under a dry nitrogen purge at the desired temperature for the desired time. Samples were placed on a flat sheet of glass fiber

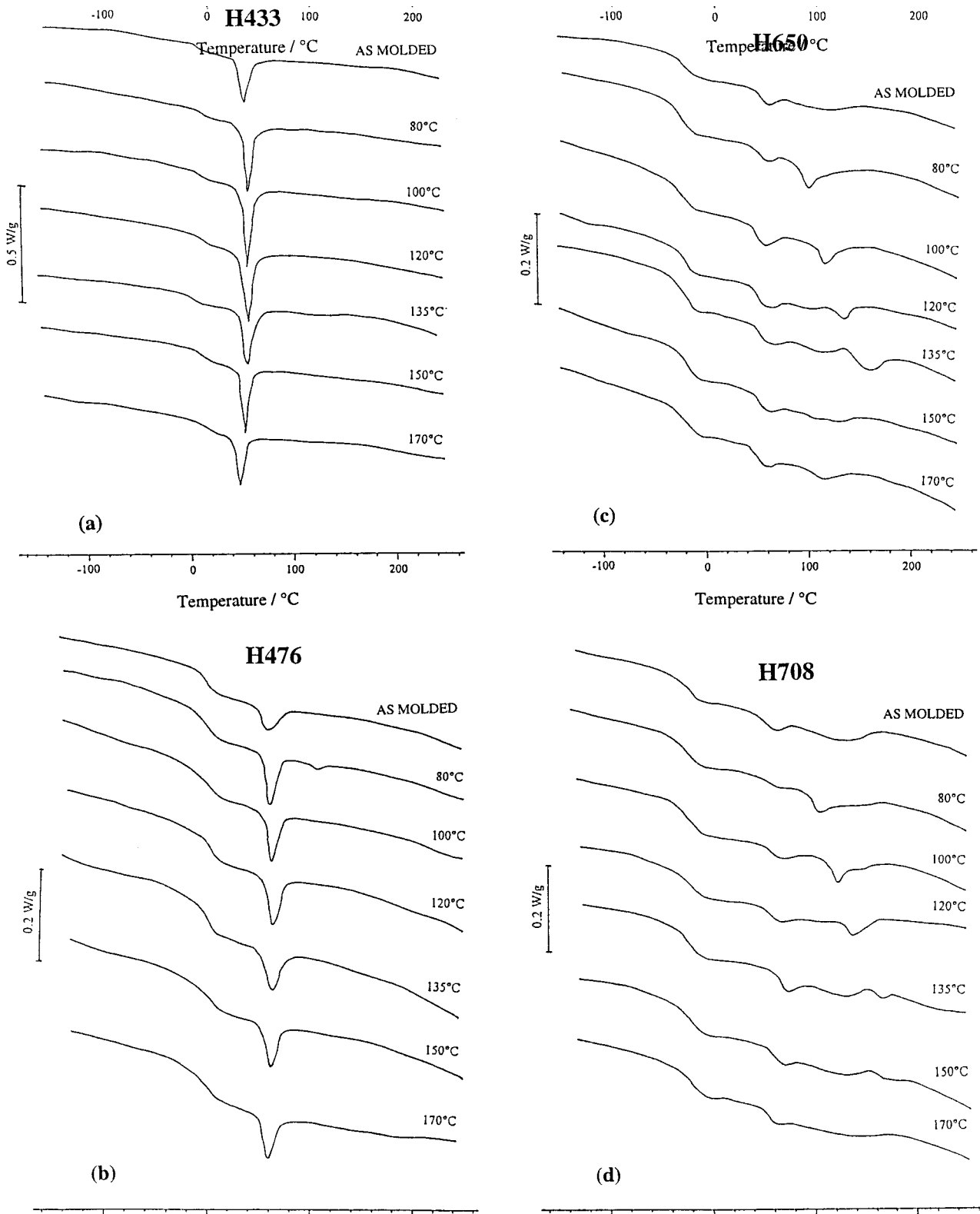


Figure 2 (a)–(h) DSC thermograms for eight polyurethane materials having undergone numerous thermal pretreatments (annealing temperatures are shown).

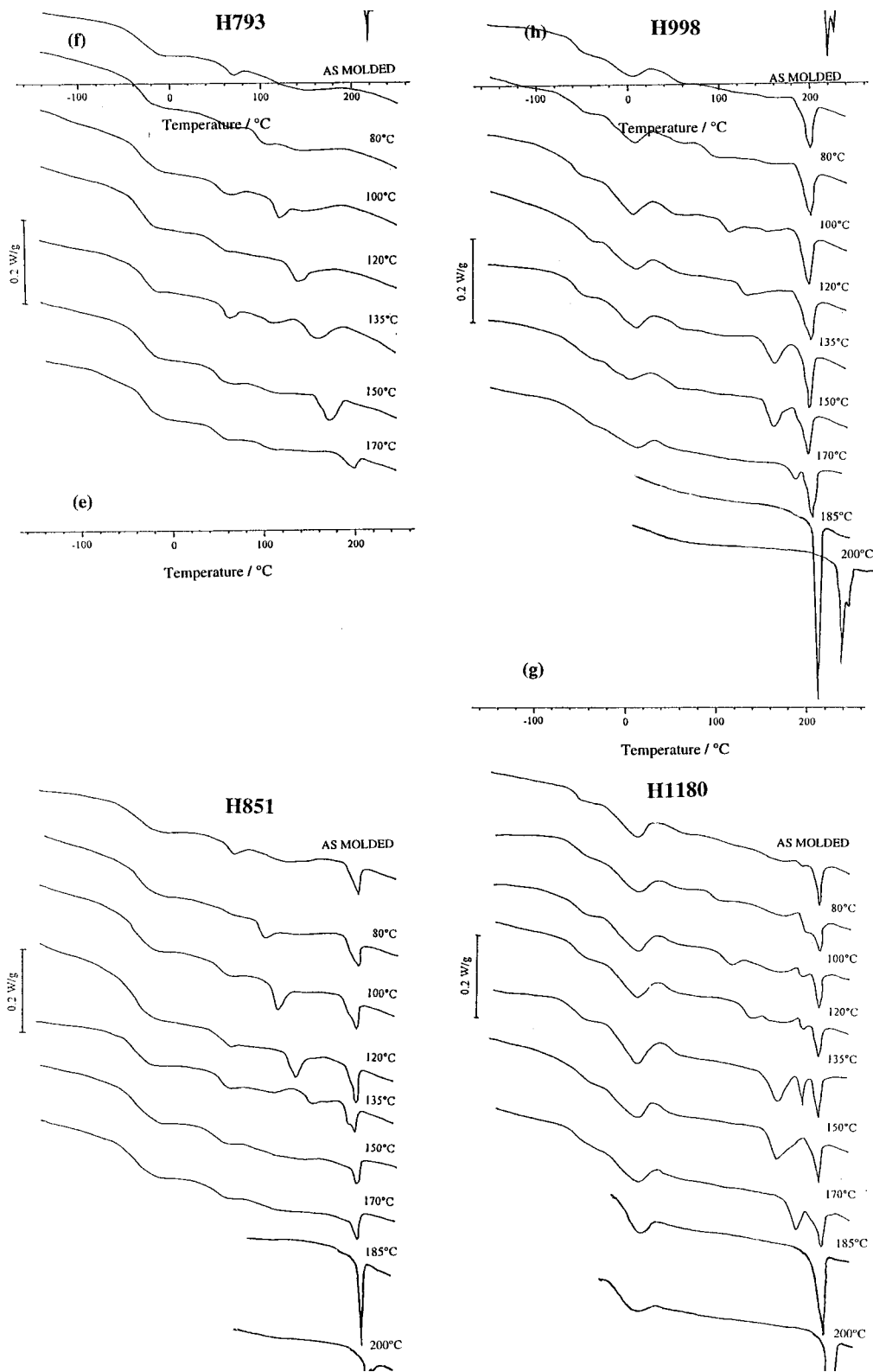


Figure 2 (Continued from the previous page)

reinforced Teflon sheet to prevent possible sticking. Annealed samples were allowed to cool to room temperature slowly in the oven.

For the series involving defined hard segment length distributions, DSC work was performed on a TA Instruments DSC2920. All other drying and run conditions were identical to above. Materials were tested in the as-synthesized and annealed states. Annealing treatments were performed on samples in DSC sample pans after cooling from the melt (250°C for 30 s) in the DSC to simulate hot pressing. The samples were annealed in their pans using the same method described above.

Small-angle x-ray scattering was performed on the SAXS facility at the Research School of Chemistry, the Australian National University, Canberra. This machine and the data processing software employed have been previously described in more detail.³⁶

Size exclusion chromatography of polyurethane samples was carried out at 80°C with 0.05 M LiBr in DMF as eluent. A Waters Associates chromatograph was employed with two μ -styrogel (10^5 and 10^3 Å) columns and one PL-gel (50 Å) column. The system was calibrated with polystyrene standards.

RESULTS AND DISCUSSION

DSC Results

Series with Variation in Average Segment Length

DSC thermograms were collected from the eight materials in this series, each having undergone seven different thermal treatments (as moulded, and annealed at 80, 100, 120, 135, 150, and 170°C for 10 h). Additional thermal treatments of 185 and 200°C are included for the three longest segment materials, H851, H998, and H1180. Figure 2(a)–(h) shows these thermograms, and Figure 3 graphically illustrates the positions of prominent melting endotherms in the study.

Five endotherms of interest are encountered in this series. These are labeled T1, T2, T3, T4, and T5 for convenience (see Fig. 3). Strong T1 endotherms are present in the two polyurethanes containing predominantly single MDI-derived units (H433 and H476), and these were attributed to melting of crystalline regions of a “fringed micelle”-type morphology, where the whole TPU chain is capable of folding and ordering in some regions. Interestingly, although the T1 DSC endotherm for H433 is quite large and sharp, the WAXD pattern for this material³⁶ indicated no crystallinity. An ab-

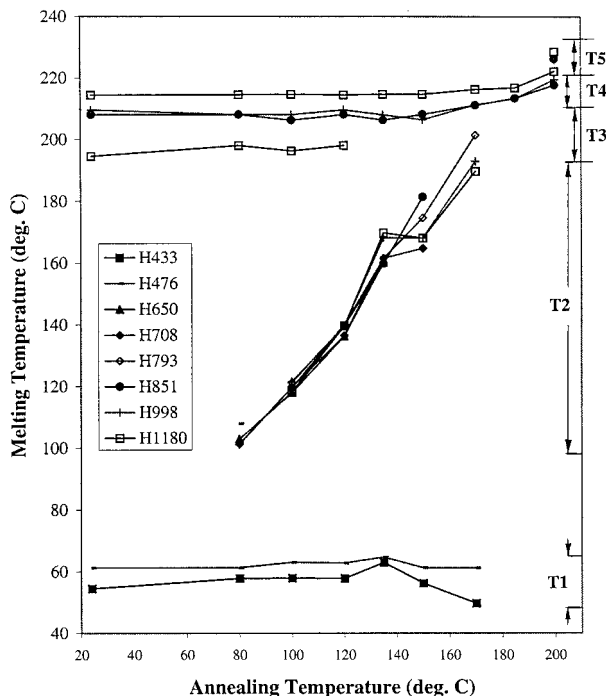


Figure 3 A graphical illustration of the positions of prominent above ambient melting endotherms with respect to annealing temperature.

sence of any SAXS scattering from this material in the same study suggested no phase separation. Hence, the T1 endotherm could be due to an interaction between adjacent single MDI-derived urethane units. Eisenbach⁵⁰ encountered DSC endotherms in the same temperature range for a “methanol–MDI–PTMO(864 MW)–MDI–methanol” compound, and attributed the endotherm to nonideally-packed N—H . . . C=O hard segment portions adjacent to the soft segment. It was suggested that in polyetherurethanes this type of structural feature could occur in the interfacial zone between the hard and soft phase. Indeed, small endotherms of this type are also observed to a decreasing extent in the longer block materials.

The T2 endotherm was of particular interest in this study because it was observed to shift upwards with increasing annealing temperature. This endotherm has been attributed to melting of agglomerations of hard segments that have an MDI–BDO–MDI structure,³⁶ and it may also involve the melting of longer hard segments, which are forced to fold because of the morphological constraints present in a material. A slight discontinuity in the sloping points in Figure 2 for the materials annealed at 135°C occurs because these materials were left to dry in the vacuum oven at 40°C for a considerably longer period of time

compared to the other samples involved. The SAXS samples annealed at 135°C also involved different aging periods and were tested on a different day to the other samples. This may account for some unexpected trends in scattering intensity also.

The T3 endotherm appears within a fixed temperature range of 195–210°C for H851 and H998. This endotherm has been assigned to the melting of crystalline regions involving MDI₃BDO₂ hard segments. Camberlin et al.⁶ reported a melting temperature of 208°C for a hard segment MDI/BDO model compound including three MDI units and end capped with ethanol. Yang reported a melting temperature of 207°C for a similar compound.^{34,35} Eisenbach⁵⁰ reported melting temperatures of approximately 192, 210, and 220°C (estimated from the figures in the citation) for BDO end-capped hard segment model compounds incorporating two, three, and four MDI-derived units, respectively. Eisenbach⁵⁰ also reported melting temperatures of approximately 169, 187, and 217°C for PTMO-based polyurethanes incorporating two, three, and four MDI-derived units in their respective monodisperse MDI–BDO hard segments. These results compare extremely well with those reported here.

A higher, T4 endotherm is present at temperatures of between 211 and 219°C for H1180 and is attributed to melting of crystalline hard domain regions involving MDI₄BDO₃ hard segments. The additional endotherms seen at 195–198°C for H1180 are thus interpreted as depressed T3 endotherms melting at slightly lower temperatures than other endotherms seen in this region due to competition for space with the more strongly bound T4 structures in H1180. For thermal treatments up to 150°C, the positions of T3 and T4 endotherms in H851, H998, and H1180 materials remain relatively constant as seen in Figure 3. As the annealing temperature is increased beyond 150°C, the T3 melting points for H851 and H998 shift to higher values and, in fact, merge with the T4 region. Similarly, the T4 points for H1180 gradually shift from around 215°C to higher values (222°C for 200°C annealing). When annealed at 200°C H851, H998, and H1180 materials produced additional melting endotherms of 226, 226, and 229°C, respectively. Endotherms in this region were named T5 endotherms.

In the same study reported above,⁵⁰ Eisenbach examined the mixing behavior of hard segment model compounds of different length by constructing phase diagrams using DSC results. The findings suggested that cocrystallization of hard

segment oligomers of varying length only occurs between oligomers of successive length and not until a critical chain length of three repeat units is exceeded. Hence, our reported T3, T4, and T5 endotherms may represent the melting of MDI–BDO crystals including three and four, four and five, and five and six MDI-derived sequences, respectively.

To clarify what affects annealing had on the molecular weight and polydispersity of the polymers with different annealing treatments, all H851, H998, and H1180 samples were examined by gel permeation chromatography (GPC). The results are presented in Figure 4(a)–(c). In all cases, the number average molecular weight of the polymers remains relatively constant for thermal treatments up to 170°C. As the annealing temperature is increased above 170°C, the molecular weight of the polymer rises sharply. In all cases the polydispersity index showed a general increase with annealing temperature. These results show that chemical changes have definitely occurred in the materials annealed at 170°C and above.

One important and very relevant phenomenon that occurs in MDI–BDO-based polyurethanes is the “*trans*-urethanization reaction,” which occurs at elevated temperatures. This was first investigated and reported by Eisenbach et al.⁵⁶ and later by Yang et al.^{34,35} Yang studied the degradation of MDI/BDO model compounds and found that the urethane bond was unstable at and above 170°C in the solid state as well as in the molten liquid state. Both chain cleavage and combination occurred to a small extent at 170°C, and significant degradation occurred above 200°C, in which case the molecular weight distribution of the originally monodisperse model compound (which included three MDI units) increased markedly to include sequences involving between 1 and 10 MDI units, as evidenced by GPC. The nondegraded model compound melted at 207°C. After thermal degradation this compound displayed melting endotherms at 190, 213, and 228°C; similar temperatures to those quoted for T3, T4, and T5 endotherms, respectively. Yang also found that the —OH-terminated model compound displayed a poorer thermal stability than the same compound end capped with phenyl isocyanate, suggesting a catalytic effect of the —OH group on degradation. Both of these compounds, however, were shown to undergo polymerization as well as depolymerization via a “*trans*-urethanization” reaction.

If we correlate the GPC results with the steady

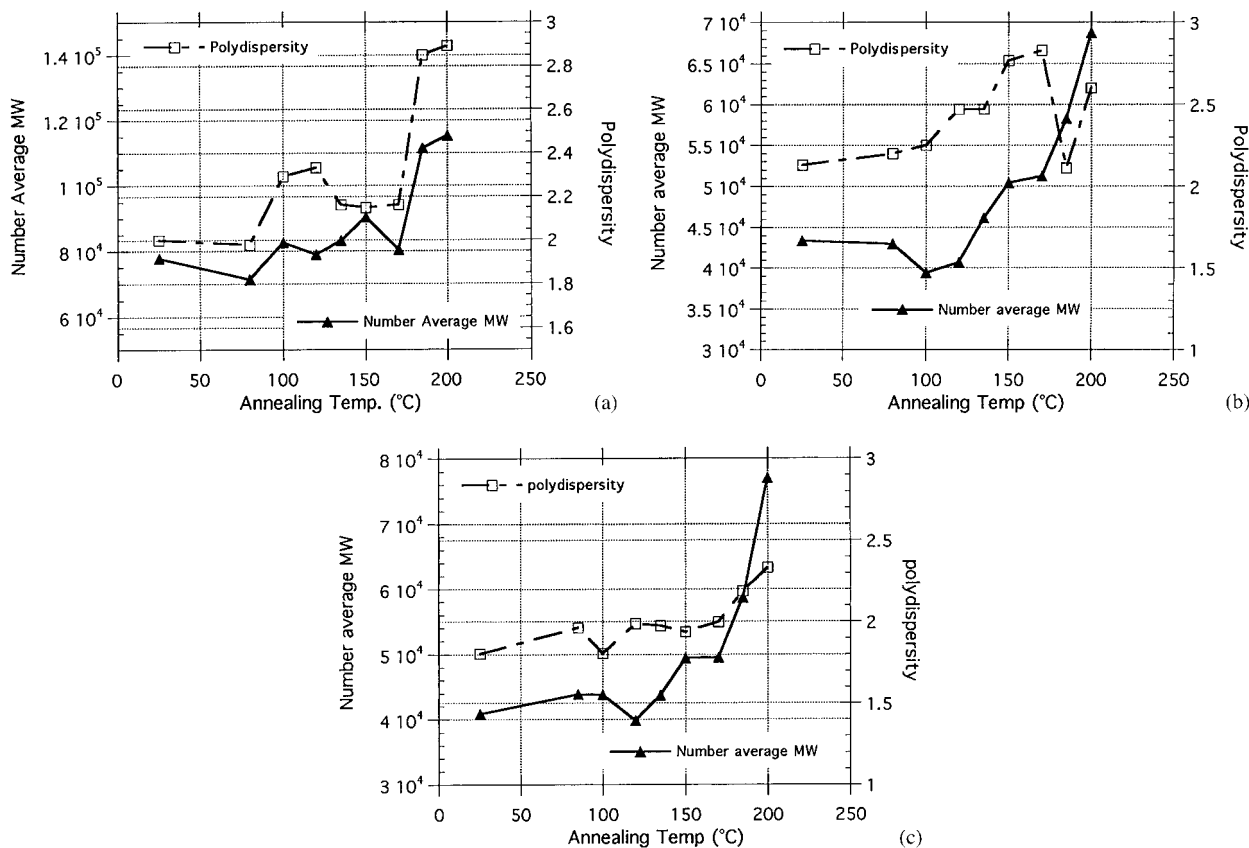


Figure 4 (a) GPC results (molecular weight and polydispersity index) with respect to annealing temperature for H851. (b) GPC results (molecular weight and polydispersity index) with respect to annealing temperature for H998. (c) GPC results (molecular weight and polydispersity index) with respect to annealing temperature for H1180.

increase in the position of T3 and T4 endotherms (and appearance of T5 endotherms for 200°C annealing temperature) as annealing temperatures were increased beyond 170°C, it seems likely that at high annealing temperatures hard segments (or MDI residues) can dissociate and recombine to produce higher melting structures while increasing the overall molecular weight of the polymer. Similarly, very long hard segments can be broken down into smaller units. For example, if at 200°C, a hard segment including about five repeat units represents the most readily crystallisable (and, therefore, most thermally stable) hard segment (see Koberstein's "partial miscibility model"^{31,39}), then the *trans*-urethanization process most likely allows for and encourages the formation of more hard segments of this length.

Series with Defined Hard Segment Length Distributions

The number average molecular weights of M2 and M3/M5 as measured by GPC were 36,300 and

30,700, respectively. Although when compared with the polymers studied in Part I of this publication these values are low, they are high enough to provide representative morphologies for the systems described. Lower molecular weights are likely to affect mechanical properties rather than morphology. The M1 polymer would not dissolve completely in DMF and, hence, its molecular weight is not given. It is not clear why this material was insoluble.

Differential Scanning Calorimetry

DSC thermograms for the as-synthesized and annealed M1, M2, and M3/M5 materials are shown in Figure 5. The nomenclature used is as follows; an "AS" suffix indicates an as-synthesized sample, and an "AXXX" suffix indicates an annealed sample, heat treated at XXX°C. Annealing treatments were 135°C for 10 h, 170°C for 2 h and 200°C for 2 h. Peak temperatures and melting enthalpy values are given in Table III. It can be seen that

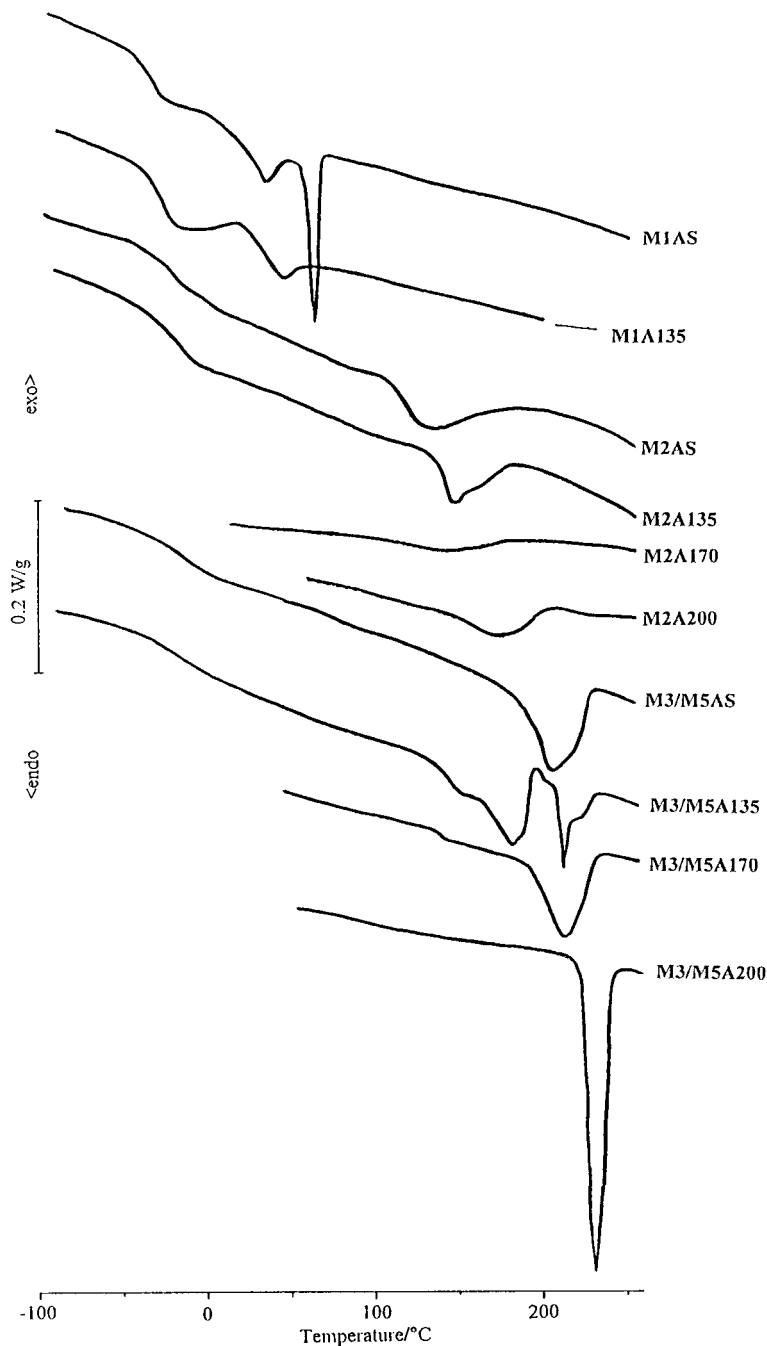


Figure 5 DSC thermograms for the as-synthesized (AS) and annealed M1, M2, and M3/M5 materials.

only hard segments that include at least three MDI residues produce melting endotherms at temperatures above 200°C. M1 shows melting behavior in the 40–70°C range (peaks seen at approximately 40°C may be due to PHMO crystallinity). The sharp melting peak seen for M1AS (as-synthesized) is believed to arise from the melting of either a fringed micelle type morphology or the

disruption of nonideally-packed single MDI-derived urethane linkages as described earlier.

The M2 polymer demonstrated a broad T₂ endotherm that shifted with annealing. The annealing temperature of 200°C was obviously above the melting point of M2, but the slow cool-down from that temperature provided ample temperature and time for hard segment ordering. It is also pos-

Table III Summary of DSC Features for the M1, M2, and M3/M5 Materials

Material	T1 Melting Peak/°C, ($\Delta H/Jg^{-1}$)	T2 Melting Peak/°C, ($\Delta H/Jg^{-1}$) ^a	T3 Melting Peak/°C, ($\Delta H/Jg^{-1}$) ^a	T5 Melting Peak/°C, ($\Delta H/Jg^{-1}$) ^a
M1AS	66.4, (10.1)	—	—	—
M1A135	42.8	—	—	—
M2AS	—	127.0, (37.7)	—	—
M2A135	—	142.8, (26.1)	—	—
M2A170	—	129.4, (10.9)	—	—
M2A200	—	166.4, (23.4)	—	—
M3/M5AS	—	—	200.7, (41.0)	—
M3/M5A135	—	175.6, (38.8)	206.4, (16.0)	—
M3/M5A170	—	—	205.3, (34.9)	—
M3/M5A200	—	—	—	233.7, (57.3)

^a Enthalpy of fusion values for hard phase melting were calculated “per gram of hard segment” rather than per gram of polymer.

sible that the hard segment sequence distribution was broadened at the high annealing temperature (*trans*-urethanization phenomena discussed earlier), thus providing some longer, higher melting hard segments. Further evidence of this is the lower melting temperature and enthalpy of fusion provided by the 170°C treatment. Earlier this T2 endotherm was attributed to an agglomeration of MDI–BDO–MDI hard segments, which were incapable of well-ordered crystallinity due to their miscibility with the soft segments. These results confirm this peak assignment.

At annealing temperatures below 200°C, the M3/M5 polyurethane exhibits a strong endotherm in the 200–206°C region. This is predominantly due to the population of hard segments incorporating 3 MDI units which have been shown in the literature to melt in this temperature range.^{6,34,35} Annealing M3/M5 at 135°C also encourages paracrystallinity between the longer M5 hard segments which, for the imposed temperature and kinetic restrictions, can only exist in the folded form, thus depressing their melting temperature. Annealing at 200°C creates a more favorable, low viscosity environment for the more thermally stable M5 hard segments to crystallize, thus producing a very large, sharp melting peak at 224°C.

Enthalpy of fusion values for the M2 and M3/M5 materials are relatively high, suggesting that the narrow hard segment sequence length distribution promotes better hard segment packing.

In the other series tested in this article, a melting endotherm was observed at 215°C for the H1180 polymer. This endotherm (“T4”) was attributed to melting of hard segments involving four MDI residues. Importantly, this endotherm does not feature in the DSC results for this series,

because these materials contain very few hard segments of this length.

It is likely that thermal dissociation and recombination of the urethane groups in these polymers occurs at temperatures above 170°C, and hence, the original hard segment length distributions in M2 and M3/M5 have probably been somewhat broadened during the melting and annealing procedures.

In any case it is probable that the hard segment length distributions in the annealed M2 and M3/M5 polymers are still narrow enough to support the “T1, T2, T3, T4, T5” hypothesis. It is also likely that this “*trans*-urethanization” plays some part in enabling higher melting hard segment structures to form when annealing temperatures of above 170°C are employed, as seen in previous sections of this article.

SAXS Results

Three of the materials were chosen for SAXS annealing testing. These were H650, H851, and H1180, because they were representative of the spread of morphologies present, and were also likely to show scattering differences with annealing. SAXS results are shown in Figures 6 and 7. Figure 6 shows the variation in average interdomain spacing values with annealing temperature for H650, H851, and H1180 materials. Figure 7 shows the variation in maximum SAXS intensity values with annealing temperature for H650, H851, and H1180 materials.

Just as the materials containing longer segments are observed to develop and sustain higher melting hard domain structures, the SAXS results show that the longer segment materials develop

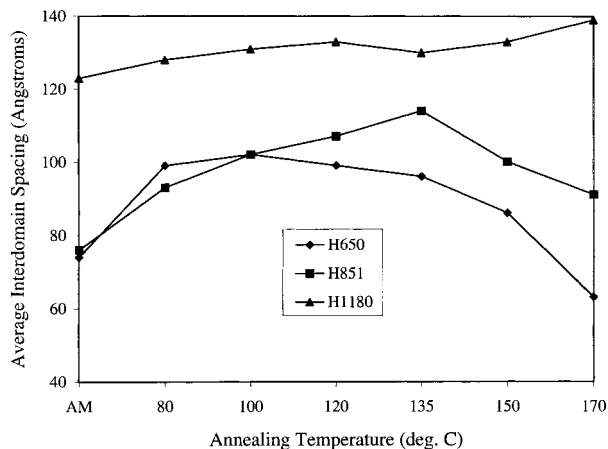


Figure 6 Variation in SAXS average interdomain spacing values with annealing temperature for H650, H851, and H1180.

maximum average interdomain spacing values at higher annealing temperatures (80, 135, and 170°C for H650, H851, and H1180, respectively, see Fig. 6).

The annealing temperatures that produced the maximum scattering intensity values were 80, 100, and 100°C for H650, H851, and H1180, respectively (see Fig. 7).

This indicated that the maximum degree of hard segment-soft segment phase separation is not necessarily related to the maximum degree of crystallinity or the maximum hard domain thickness, and that at annealing temperatures above 100°C, many of the shorter hard segments are soluble in the soft domains.

CONCLUSIONS

Five DSC melting endotherms of interest were encountered in the series involving variations in average segment length. These were labeled T1 (50–70°C), T2 (100–180°C), T3 (190–210°C), T4 (211–217°C), and T5 (222–230°C). The results provided strong evidence to suggest that these five endotherms were a result of the disordering of structures including predominantly single MDI-derived sequences, MDI₂BDO, MDI₃BDO₂, MDI₄BDO₃, and MDI₅BDO₄ hard segments, respectively. It was also proposed that the sometimes broad T2 endotherm may also be associated with the disordering of folded, longer hard segments.

An annealing-induced increase in average hard segment length via dissociation and recombination of urethane linkages (or “*trans-*

urethanization”) was thought to be the cause of molecular weight and melting temperature increases for annealing temperatures above 170°C. This process had the effect of increasing hard domain melting temperatures by enabling more T4 and/or T5 structures to form (in H851, H998, and H1180) and was evidenced by a sharp increase in molecular weight with annealing above 170°C.

An increase in segment length provides microstructures that are able to develop and sustain, more cohesive, higher melting hard domain structures. Similarly, longer segment materials attain maximum average interdomain spacing values at higher annealing temperatures.

For phase-separated materials in this series, an annealing temperature of 80–100°C enabled the maximum degree of phase separation, as indicated by the maximum SAXS intensity. This result suggested that at annealing temperatures above 100°C, many of the shorter hard blocks are soluble in the soft domains.

This article has provided information to suggest that the multiple endothermic behavior encountered for compression-molded MDI–BDO polyetherurethanes may be due to the melting of various hard segment length populations. The characterization of a series of polyurethanes prepared with quite narrow hard segment length distributions has served to reinforce this hypothesis.

Where kinetic or thermodynamic barriers (temperature, time, or solubility) prevent the extended alignment of long hard segments, these hard segments fold into a paracrystalline arrangement that contributes to the “T2” melting region (100–180°C).

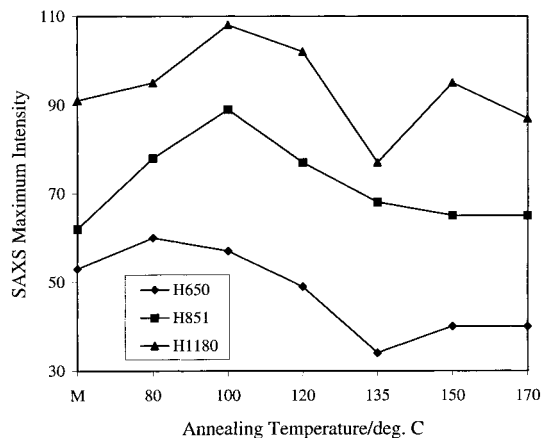


Figure 7 Variation in maximum SAXS intensity values with annealing temperature for H650, H851, and H1180.

This work provides practical support for Koberstein and Russel's morphological model, which explains that for a given annealing temperature there will be a tendency for intermediate-length sequences to crystallize preferentially.³¹

It is probable that for annealing temperatures above 170°C that "trans-urethanization" plays some part in enabling higher melting hard segment structures to form.

REFERENCES

- J. Foks, H. Janik, and R. Russo, *Eur. Polym. J.*, **26**, 309 (1990).
- R. Russo, *Colloid Polym. Sci.*, **269**, 1 (1991).
- K. Sreenivasan, *Eur. Polym. J.*, **27**, 811 (1991).
- X. Yuying, Z. Zhiping, W. Dening, and Y. Shengkang, *Polymer*, **33**, 1335 (1992).
- J. Blackwell and C. D. Lee, *Advances in Urethane Science and Technology*, K. C. Frisch and D. Klemperer, Eds., Technomic, Stamford, Conn., 1984).
- Y. Camberlin, J. P. Pascault, M. Letoffe, and P. Claudy, *J. Polym. Sci., Polym. Chem. Ed.*, **20**, 383 (1982).
- T. R. Hesketh, J. W. C. Van Bogart, and S. L. Cooper, *Polym. Eng. Sci.*, **20**, 190 (1980).
- W. Hu and J. T. Koberstein, *J. Polym. Sci., Polym. Phys. Ed.*, **32**, 437 (1994).
- J. T. Koberstein and A. F. Galambos, *Macromolecules*, **25**, 5618 (1992).
- J. W. C. Van Bogart, D. A. Bluemke, and S. L. Cooper, *Polymer*, **22**, 1428 (1981).
- J. W. C. Van Bogart, P. E. Gibson, and S. L. Cooper, *J. Polym. Sci., Polym. Phys. Ed.*, **21**, 65 (1983).
- T. G. Fox, *Bull. Am. Phys. Soc.*, **50**, 549 (1956).
- L. A. Wood, *J. Polym. Sci.*, **28**, 319 (1958).
- S. C. Yoon and B. D. Ratner, *Macromolecules*, **21**, 2392 (1988).
- N. S. Schneider, C. S. Paik Sung, R. W. Matton, and J. L. Illinger, *Macromolecules*, **8**, 62 (1975).
- Z. S. Petrovic and I. Javni, *J. Polym. Sci., Polym. Phys. Ed.*, **27**, 545 (1989).
- R. W. Seymour and S. L. Cooper, *Polym. Lett.*, **9**, 695 (1971).
- K. B. Wagener, *Macromolecules*, **25**, 5591 (1992).
- M. E. Kazmierczak, R. E. Fornes, D. R. Buchanan, and R. D. Gilbert, *J. Polym. Sci., Polym. Phys. Ed.*, **27**, 2188 (1989).
- L. M. Leung and J. T. Koberstein, *Macromolecules*, **19**, 706 (1986).
- J. A. Miller, S. B. Lin, K. K. S. Hwang, K. S. Wu, P. E. Gibson, and S. L. Cooper, *Macromolecules*, **18**, 32 (1985).
- W. Meckel, W. Goyert, and W. Weider, *Thermoplastic Elastomers*, N. R. Legge, L. Holden, and H. E. Schroeder, Eds., Hanser, Munich, New York, 1987.
- S. B. Clough, N. S. Schneider, and A. O. King, *J. Macromol. Sci.*, **B2**, 641 (1968).
- S. L. Samuels and G. L. Wilkes, *J. Polym. Sci., Polym. Symp.*, **43**, 149 (1973).
- R. W. Seymour and S. L. Cooper, *Macromolecules*, **16**, 48 (1973).
- C. S. Paik Sung and N. S. Schneider, *Macromolecules*, **8**, 68 (1975).
- C. S. Paik Sung, C. B. Hu, and C. S. Wu, *Macromolecules*, **13**, 111 (1980).
- R. Wildnauer and G. L. Wilkes, *Am. Chem. Soc., Div. Polym. Chem. Polym. Prepr.*, **6**, 600 (1975).
- G. L. Wilkes, S. Bagrodia, W. Humphries, and R. Wildnauer, *Polym. Lett.*, **13**, 321 (1975).
- G. L. Wilkes and R. Wildnauer, *J. Appl. Phys.*, **46**, 4148 (1975).
- J. T. Koberstein and T. P. Russel, *Macromolecules*, **19**, 714 (1986).
- C. D. Eisenbach and C. Gunter, *Polym. Prepr.*, **26**(2), 7 (1985).
- K. K. S. Hwang, G. Wu, S. B. Lin, and S. L. Cooper, *J. Polym. Sci., Polym. Chem., Ed.*, **22**, 1677 (1984).
- W. P. Yang, C. W. Macosko, and S. T. Wellinghoff, *ACS Polym. Prepr.*, **26**, 321 (1985).
- W. P. Yang, C. W. Macosko, and S. T. Wellinghoff, *Polymer*, **27**, 1235 (1986).
- D. Martin, G. F. Meijjs, G. M. Renwick, S. J. McCarthy, and P. A. Gunatillake, *J. Appl. Polym. Sci.*, to appear.
- Annual Book of ASTM Standards*, 1975.
- C. P. Christenson, M. A. Harthcock, M. D. Meadows, H. L. Spell, W. L. Howard, M. W. Creswick, R. E. Guerra, and R. B. Turner, *J. Polym. Sci., Polym. Phys. Ed.*, **24**, 1401 (1985).
- J. T. Koberstein and R. S. Stein, *J. Polym. Sci., Polym. Phys. Ed.*, **21**, 1439 (1983).
- L. H. Peebles, Jr., *Macromolecules*, **7**, 872 (1974).
- L. H. Peebles, Jr., *Macromolecules*, **9**, 58 (1976).
- J. J. Dumais, L. W. Jelinski, L. M. Leung, I. Gancarz, A. Galambos, and J. T. Koberstein, *Macromolecules*, **18**, 116 (1985).
- A. Kintanar, L. W. Jelinski, I. Gancarz, and J. T. Koberstein, *Macromolecules*, **19**, 1876 (1986).
- J. Blackwell and C. D. Lee, *J. Polym. Sci., Polym. Phys. Ed.*, **22**, 759 (1984).
- R. M. Briber and E. L. Thomas, *J. Macromol. Sci., Phys.*, **B22**, 509 (1983).
- R. M. Briber and E. L. Thomas, *J. Polym. Sci., Polym. Phys. Ed.*, **23**, 1915 (1985).
- L. Born, J. Chroné, H. Hespe, E. H. Muller, and K. H. Wolf, *J. Polym. Sci., Polym. Phys. Ed.*, **22**, 163 (1984).
- C. M. Brunette, S. L. Hsu, W. J. MacKnight, *Macromolecules*, **15**, 71 (1982).
- J. Blackwell and C. D. Lee, *J. Polym. Sci., Polym. Phys. Ed.*, **21**, 2169 (1983).

50. C. D. Eisenbach, M. Baumgartner, and C. Gunter, *Advances in Elastomers and Rubber Elasticity*, J. Lal and J. E. Mark, Eds., Plenum, New York, 1986.
51. W. Kern, K. J. Rauterkis, and H. Sutter, *Makromol. Chem.*, **44**, 78 (1961).
52. L. L. Harrel, Jr., *Macromolecules*, **2**, 607 (1969).
53. Z. Y. Qin, C. W. Macosko, and S. T. Wellinghoff, *Proc. Div. Polym. Mater. Sci. Eng.*, **49**, 475 (1983).
54. Z. Y. Qin, C. W. Macosko, and S. T. Wellinghoff, *Macromolecules*, **18**, 553 (1985).
55. D. J. Martin, G. F. Meijs, G. M. Renwick, P. A. Gunatillake, and S. J. McCarthy, *J. Appl. Polym. Sci.*, **60**, 557 (1996).
56. C. D. Eisenbach, C. Gunter, M. Baumgartner, and U. Struth, *Makromol. Colloquium*, Preiburg, February 1984.
57. Y. P. Chang and G. L. Wilkes, *J. Polym. Sci., Polym. Phys. Ed.*, **13**, 455 (1975).
58. M. A. Vallance, J. L. Castles, and S. L. Cooper, *Polymer*, **25**, 1734 (1984).